Marine and Petroleum Geology 25 (2008) 681–695

Contents lists available at ScienceDirect

Marine and Petroleum Geology

journal homepage: www.elsevier.com/locate/marpetgeo

Diagenesis and reservoir quality of Miocene sandstones in the Vienna Basin, Austria

Susanne Gier [a,*], Richard H. Worden [b], William D. Johns [c], Hans Kurzweil [a]

[a] Department of Geodynamics and Sedimentology, University of Vienna, Althanstrasse 14, A-1090 Wien, Austria
[b] Department of Earth and Ocean Sciences, University of Liverpool, 4 Brownlow Street, Liverpool L69 3GP, UK
[c] Department of Geological Sciences, University of Missouri, Columbia, MO 65211, USA

ARTICLE INFO

Article history:
Received 30 May 2008
Accepted 3 June 2008

Keywords:
Sandstone diagenesis
Reservoir quality
Carbonate cement
Quartz cement
Ductile lithic grains
Compaction
Illite–smectite ratio
Vienna Basin

ABSTRACT

A study of the diagenetic evolution of Neogene sandstones in the Vienna Basin (Austria) was undertaken to unravel the controls on reservoir quality. These rocks present a ~2000 m succession of relatively similar lithic arkoses with the deepest rocks buried progressively to nearly 3000 m and thus present an opportunity to study sequential diagenetic changes. The Neogene sandstones sit above Alpine allochthonous nappes and autochthonous Mesozoic sediments that include Jurassic source rocks. Oil has been produced from Badenian marine sandstones at about 1700 m but reservoir quality is marginal. Thirty-eight samples from 892 m to 2774 m were studied using petrography, XRD, SEM, microprobe, infrared spectroscopy and a range of modelling approaches. The sandstones contain abundant ductile grains and a variety of carbonate grains. The main eogenetic cements include clay coats, pyrite and possibly glauconite. The main mesogenetic cements include the dominant calcite, kaolinite and minor quartz. Smectite was replaced predominantly by illite with minor growth of grain-coating chlorite. Thermal histories for each sandstone sample were calibrated by modelling the degree of smectite to illite transformation. These sample-specific thermal histories were then used to model quartz precipitation revealing that quartz cement, the most important cement in many sandstones worldwide, is of negligible significance here because (1) there has been insufficient time since deposition, or (2) the geothermal gradient is not high enough or (3) calcite cement filled the pore space before quartz cement could grow. Instead porosity has been controlled by the abundance of detrital ductile (lithic) grains and the abundance of detrital carbonate grains which have been variably dissolved and reprecipitated as ferroan calcite cement. The highest porosity for a given depth decreases with increasing depth due to compactional processes. Porosity is highest for samples where both the detrital ductile grain and carbonate cement contents are low. The accumulation of oil in the middle part of the section has had no discernable effect on porosity since diagenesis is mostly controlled by compactional and carbonate recrystallisation processes and oil probably entered the reservoir late in the diagenetic sequence, after ductile compaction and growth of carbonate cements had already occurred.

1. Introduction

Reservoir quality is one of the key controls on prospectivity during petroleum exploration. It is important to have a detailed understanding of what controls reservoir quality to assist with the appraisal of the economic viability of petroleum discoveries. When a petroleum discovery has been made in a basin, it is essential to gain as much understanding of reservoir quality to help focus further exploration and appraisal efforts (Selley, 1997).

As far as clastic sediments are concerned, the first control on reservoir quality is primarily a function of the basic presence of sand as opposed to silt or mud. However, during burial the deposited sand never retains its original porosity, fabric or even mineralogy as it becomes sandstone (Worden and Burley, 2003). During exploration, remote sensing techniques and analogue studies can help to identify the presence of sandstone but they do not usually help to find high porosity sandstones that have been preserved from major diagenetic alteration and porosity-loss. It is essential to study core samples to understand what diagenetic changes have occurred and what has controlled reservoir quality.

Diagenesis comprises a broad spectrum of physical, geochemical and biological post-depositional processes by which original sedimentary mineral assemblages and their interstitial pore waters interact in an attempt to reach textural and thermodynamic equilibrium with their environment (Worden and Burley, 2003).

* Corresponding author.
E-mail address: susanne.gier@univie.ac.at (S. Gier).

0264-8172/$ – see front matter © 2008 Elsevier Ltd. All rights reserved.
doi:10.1016/j.marpetgeo.2008.06.001

Diagenetic processes that occur in the earlier stages of a burial cycle are collectively known as "eodiagenesis" while processes that occur after eodiagenesis are collectively called "mesodiagenesis" (also commonly called burial diagenesis). Eodiagenesis has been defined in two ways: either (1) those processes that occur when sediment is close to the surface and in communication with surface-supplied oxygenated water (Burley, 1984; Worden and Burley, 2003), or (2) those processes that occur when a sediment has been buried to less than about 2000 m, usually equivalent to less than about 70 °C (Morad et al., 2000). For most sandstones, the difference in definition of eodiagenesis is relatively unimportant since after burial to a few hundred metres relatively few cementation and mineral alteration processes occur until a rock reaches temperatures of >70 °C when it has been buried to a few thousand metres.

Processes that occur during diagenesis fall into three categories: compaction, mineral precipitation, and mineral dissolution. Alteration of detrital grain and minerals could also be added but, in essence, this is a special case of sequential dissolution and precipitation at the same site (Worden and Burley, 2003). Compaction includes mechanical compaction (rearrangement of grains) and chemical compaction (also known as pressure dissolution). Diagenesis is characterized by rock-fluid systems that are out of geochemical and textural equilibrium and so it is the study of the kinetics of processes that presents the greatest challenges to diagenesis and reservoir quality research. In other words, what are the rates of the various processes (e.g. cementation, mineral alteration) that occur during diagenesis? If it was possible to understand and then model the kinetics of diagenetic processes then it starts to become possible to quantitatively predict reservoir quality distribution in the subsurface. However, there are many unresolved controversies about practically every aspect of sandstone diagenesis. There are different and opposing schools of thought applied to everything from the origin and timing of clay mineral coats on sand grains in sandstones (Needham et al., 2004, 2005; Worden and Morad, 2003), the timing, kinetics and mode of quartz cementation (Haszeldine et al., 2000; Walderhaug et al., 2000; Worden and Morad, 2000), and the effect of petroleum emplacement on diagenesis (De Souza and De Assis Silva, 1998; Ehrenberg and Jakobsen, 2001; Worden et al., 1998; Yurkova, 1970).

There are many problems with achieving the ability to model sandstone diagenesis and predict reservoir quality including poorly defined kinetic constants for most diagenetic processes. Use of empirical datasets has started to help develop kinetic models for some of the simpler diagenetic processes (e.g. Walderhaug et al., 2000; Wei et al., 1996).

In this paper we report a study of reservoir quality evolution in a suite of Neogene sandstones from a well (Aderklaa-78) in the Vienna Basin, Austria that was continuously cored down to 2800 m. These rocks have had a relatively simple thermal and burial history and provided the opportunity to examine the evolution of diagenesis and reservoir quality during burial and assess the rates of several important key processes. Specifically we seek to answer the following questions:

(1) What diagenetic processes occurred in these fluvial to marine Neogene sandstones during burial?
(2) What are the most volumetrically important mineral cements?
(3) What controls reservoir quality?
(4) Has oil emplacement had any discernable influence on sandstone diagenesis?

2. Geological background

The Vienna Basin is located in the northeast part of Austria (Fig. 1). It is a 200 km long and 60 km wide pull-apart basin along the junction of the Eastern Alps and the Western Carpathians. Evolution of the basin started during the early Miocene with subsidence along northeast trending sinistral faults (Wagreich and Schmid, 2002).

The basement of the Vienna basin is formed by the Hercynian Bohemian Massif and its autochthonous sedimentary cover of Lower Jurassic to Upper Creatceous (Ladwein, 1988). Thrusted above this autochtonous cover are allochthonous Alpine nappes which were transported from the south. These allochthonous sedimentary rocks were deformed during thrusting; rocks from the Northern Calcareous Alps are Permian to Cretaceous while strata from the Flysch Zone are Lower Cretaceous to Eocene.

Sitting above the allochthonous and deformed sediments are the Neogene sedimentary rocks of the Vienna Basin dominated by sandstones, marls and, to a lesser extent, carbonates. The Neogene part of the succession can exceed 5000 m in thickness in the depocenters (Ladwein, 1988). The Karpatian sediments, at the base of the Neogene part of the section, were deposited in a lacustrine to fluvial environment. A marine transgression started in the early Badenian. The marine environment of the Badenian evolved to brackish water conditions during the Sarmatian and with continuing decrease in salinity, leading to lacustrine and fluvial deposits in the Pannonian (Sauer et al., 1992).

The Badenian reservoir rocks in the Neogene part of the succession are transgressive sandstones although pay zones have also been found in fractured Triassic dolomites in the allochthonous nappes below the Neogene basin fill. Reservoirs in the autochthonous Mesozoic have been suspected in dolostones and deltaic sandstones (Ladwein, 1988).

Oil and gas have been produced from the Neogene reservoirs in the Vienna Basin since the 1930s. Aderklaa-78 (Figs. 1 and 2) was drilled in 1958 by OMV AG, in the course of which oil was discovered and subsequently produced from the Badenian (Upper Lagenid Zone) sandstones at about 1700 m. The drilling of Aderklaa-78 involved continuous coring and is therefore especially useful for carrying out burial diagenetic investigations. The diagenetic developments of the interbedded shales were the subject of previous extensive studies (Horton et al., 1985; Johns and Kurzweil, 1979; Kurzweil and Johns, 1981).

The Upper Jurassic (Malmian) marls in the pre-Neogene, autochthonous part of the section have been identified as the main petroleum source rocks in the Vienna Basin (Hamilton et al., 1999). The main phase of oil generation has been shown by pyrolysis to occur in the autochthonous strata below the Neogene succession between depths of 4000 m and 6000 m (Ladwein, 1988). The geothermal gradient in the basin is spatially variable but the area near the well in question has a current geothermal gradient of 30 °C/km and seems to have been broadly uniform since deposition (Sachsenhofer, 2001). Thermal and burial histories of the base for the Miocene Badenian sediments and the oil-bearing sandstones at 1700 m have been constructed based on the geothermal gradient stated and the burial history of a nearby well (Wagreich and Schmid, 2002; Fig. 3)

3. Methods

Thirty-eight sandstone samples from the Aderklaa-78 well in the Vienna Basin were collected from 892 to 2774 m (Fig. 2). Samples were impregnated with blue resin before thin sectioning in order to indicate porosity. Thin sections were stained with Alizarin Red S and K-ferricyanide for carbonate mineral determination. Sandstone modal composition was determined from all thin sections of medium to coarse-grained sandstones by counting 300 points per thin section.

For clay mineral investigation, the <2 μm-fractions were separated from the sandstones and the mineralogical compositions

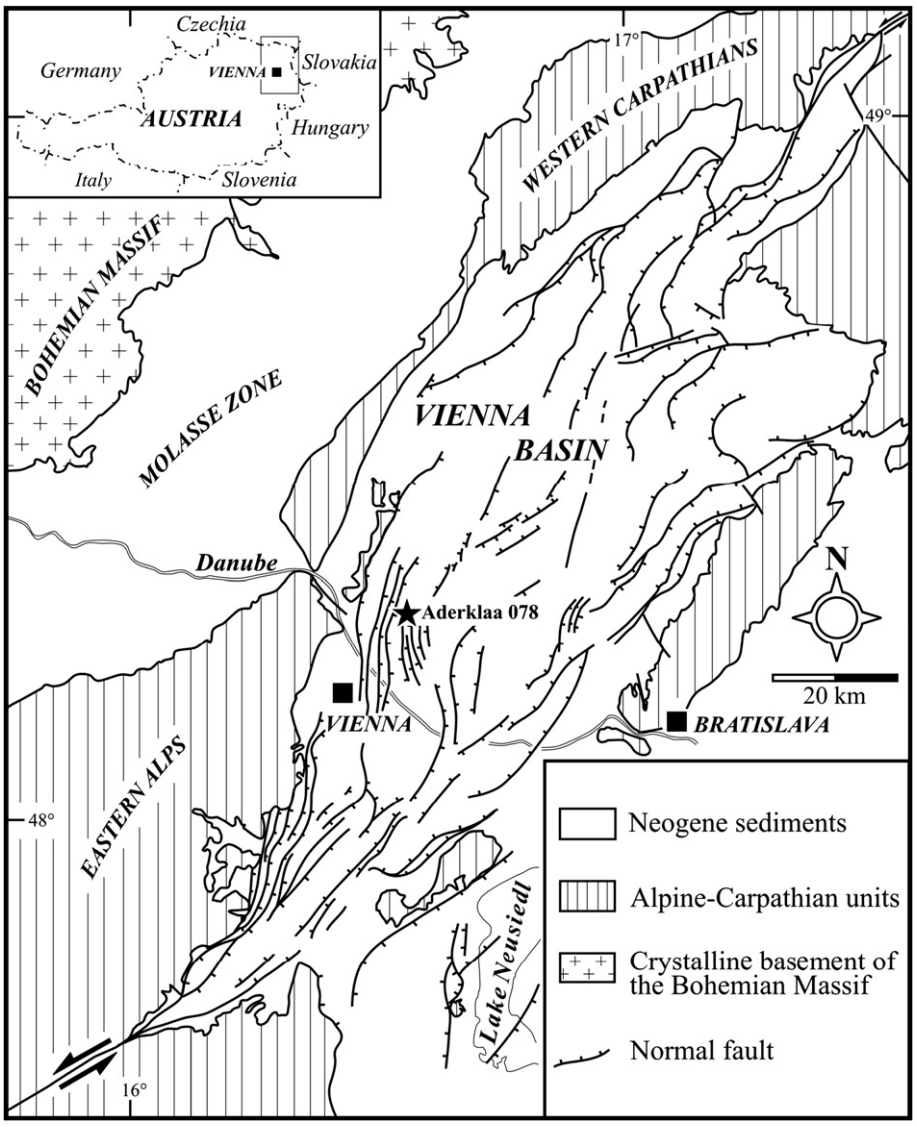

Fig. 1. Regional geological map and the position of the well Aderklaa-78 (adapted from Wagreich and Schmid, 2002).

were determined by X-ray diffraction analyses (XRD), using a Philips (PW 3710) diffractometer (Cu Kα radiation, 45 kV, 35 mA). For the purpose of separation of the clay fraction, the outer rim (approximately 5 mm) of each core was removed to avoid possible contamination from drilling mud. Afterwards the sandstones were crushed to 2 mm pieces, disaggregated with diluted H_2O_2 and treated with a 400 W ultrasonic probe (2 × 3 min). The <2 μm fractions were obtained by sedimentation. The samples containing carbonates were treated with a 0.1 M EDTA solution (pH 4.5) and then washed with distilled water. Oriented XRD mounts were prepared by pipetting the clay suspensions (7 mg/ml) onto glass slides, and were analysed after air-drying and after vapor saturation with ethylene glycol at 60 °C for 12 h. The proportions of smectite and illite in the I/S phase were determined using the 2-theta method described by Moore and Reynolds (1997).

FT-IR analysis was performed using a Nicolet 380 FT-IR spectrometer. Samples of the <2 μm-fraction of each sample were diluted with analytical grade KBr to create a 0.5% mixture. This KBr-sample mixture was then subjected to 10 tonnes of pressure using a Specak press in order to create a solid disc. All samples were heated for 18 h in an oven at 160 °C (e.g. Zviagina et al., 2004) to remove the majority of the free water (~3350–3650 cm^{-1}) in order to help resolution of clay-hydroxyl bands (~3500–3700 cm^{-1}). This process does not alter clay minerals or organics yet has a significant benefit during interpretation of the IR spectra. Each disk was analysed in transmission mode with a single analysis integrating 64 scans at a resolution of 4 cm^{-1}. The output from all samples was recorded in absorbance units, later calibrated against standards, and was analysed using Omnic software (Nicolet Instruments Corporation). All spectra had background subtracted; peak deconvolution performed of the clay-hydroxyl (3450–3750 cm^{-1}) and the $-CH_2$ and $-CH_3$ (−3000 to 2800 cm^{-1}) regions of the spectrum. Deconvolution was performed using Omnic based on a Gaussian model and using a full width-half height ratio of ten. To quantify the amounts of kaolinite, calibration standards of pure kaolinite were prepared diluted in analytical grade KBr at 0.1% and 0.5%. The area of the deconvoluted kaolinite 3699 cm^{-1} peak was measured for all samples and compared to the areas of the deconvoluted 3699 cm^{-1} peaks for the two standards to quantify the kaolinite from FT-IR spectra. A related approach was used to quantify illite–smectite. Kaolinite can be quantified using the 3699 cm^{-1} band since no other clay minerals have bands of that wavenumber. Illite and smectite have dominant bands at 3620 cm^{-1} but this is not unique since kaolinite also

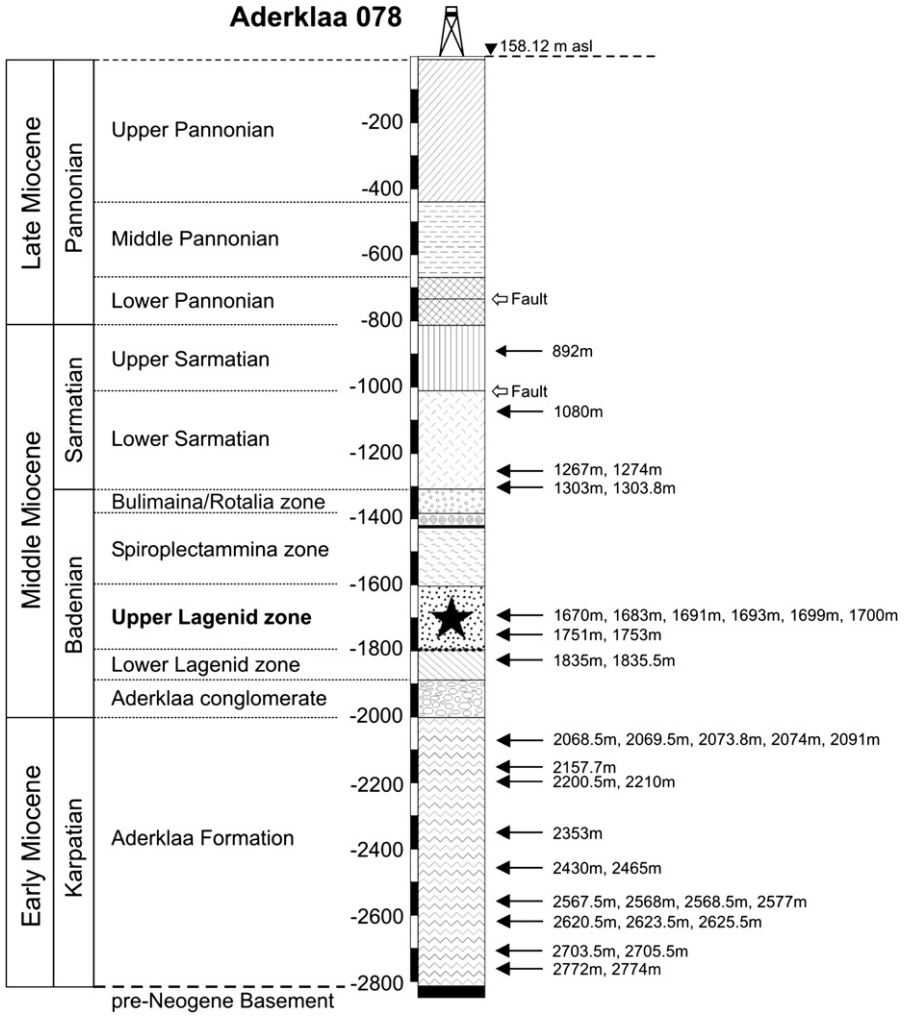

Fig. 2. Stratigraphic column from well Aderklaa-78 and the positions of the investigated core samples. Zone of petroleum occurrence is marked with a star.

contributes to the 3620 cm^{-1} band. The kaolinite 3620 cm^{-1} band has half the area of its 3699 cm^{-1} band so that subtracting half the 3699 cm^{-1} band intensity from the total 3620 cm^{-1} band intensity leaves only the area contribution from the illite and smectite minerals. If it is assumed that the illite and smectite minerals have the same response factor to IR absorption as kaolinite then the kaolinite calibration can be applied to the aggregate of I/S minerals.

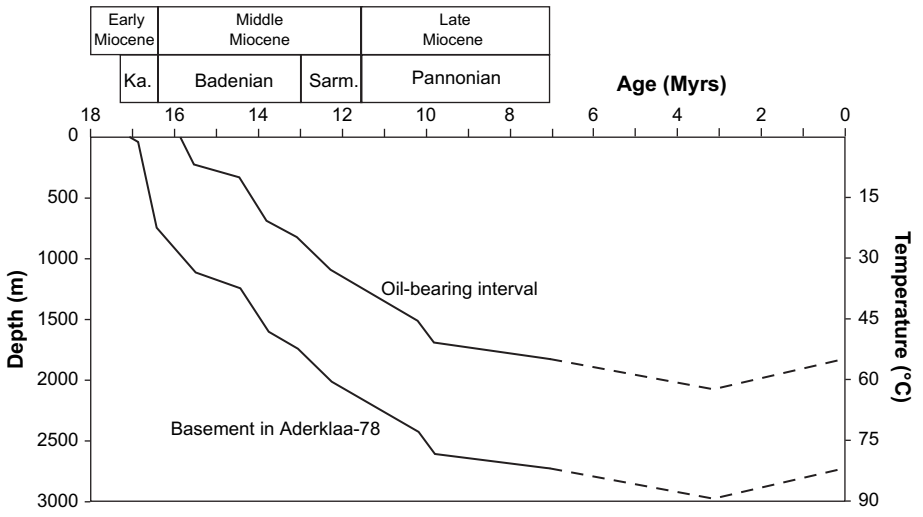

Fig. 3. Burial curve illustrating the evolution of the basin (modified from Wagreich and Schmid, 2002).

Polished thin sections were prepared for the purpose of cathodoluminescence (CL) and electron microprobe analysis. CL analysis was carried out using a CITL Cold Cathode Luminescence 8200 mk3, excitation energy 20 kV and 400 μA. A Cameca SX100 electron microprobe was used to analyze the chemical compositions of diagenetic calcite, using 15 kV acceleration voltage, 10 nA sample current, and 5 μm beam diameter.

The textural studies of the cements in the sandstone samples were performed on fractured surfaces, coated with gold on a Philips XL 30 ESEM scanning electron microscope (SEM).

4. Results

4.1. Sandstone petrology: detrital mineralogy

The Aderklaa-78 Miocene sandstones are fine to coarse-grained. The sandstones are generally texturally immature. Sorting ranges from poor to well sorted. The roundness of the detrital grains varies from angular to subangular.

The Miocene sandstones are mostly lithic arkoses to feldspathic litharenites and subarkoses (Figs. 4–6; Folk, 1968). The average framework composition of the sandstones is $Q_{60}F_{22}L_{18}$. In general, the total feldspar proportion does not vary systematically with depth but there are a few samples in the deeper Karpatian section that are strongly arkosic, with a K-feldspar content of up to 24% (Fig. 8c). The (non-carbonate, see later) lithic grain content seems to slightly decrease in abundance up the stratigraphic section (Karpatian, 23.4%; Badenian, 19.7%; Sarmatian, 17.1%). The variation of ductile grain (plastically deformable grain) content with depth of burial is displayed in Fig. 7.

The majority of the detrital quartz grains are monocrystalline. The detrital feldspars in these sandstones are mostly variably altered K-feldspars (Fig. 5a–c). Altered feldspars are commonly associated with kaolin.

The form of carbonate minerals in these rocks seem to evolve with burial being pore-filling cement in the deeper section (see later) but are clearly detrital (bioclastic and carbonate rock fragments) in the shallower section. The point-counted lithic totals (e.g. the overall average: $Q_{60}F_{22}L_{18}$) do not include carbonate minerals even though in the shallower section some carbonates were indeed lithic fragments. Much of the rock fragment population is sedimentary in origin, consisting of limestone and dolostone grains. However, it proved impossible in practice to unequivocally discriminate bioclastic debris, limestone and dolostone rock fragments and carbonate cement so these have been grouped together and labelled total carbonate.

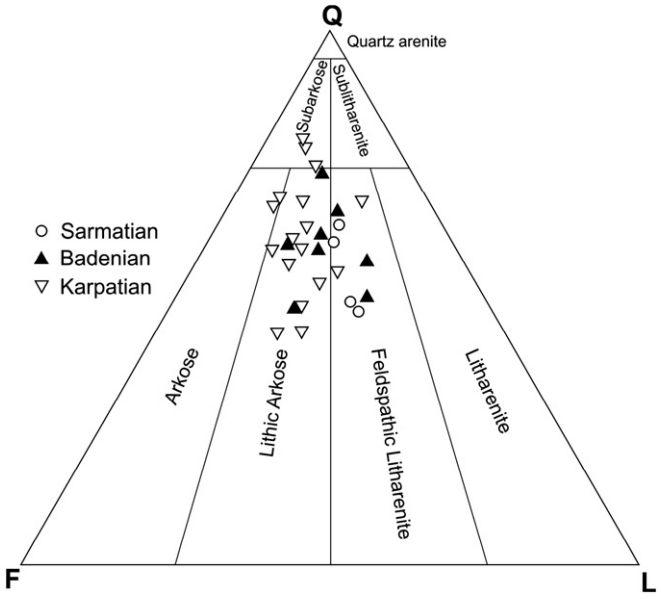

Fig. 4. QFL classification of Aderklaa-78 sandstones (after Folk, 1968).

4.2. Sandstone petrology: diagenetic mineralogy

Authigenic minerals are dominated by combinations of calcite, quartz, illite, illite/smectite, kaolinite, chlorite with minor amounts of framboidal pyrite and glauconite.

Thin clay coats surround some detrital grains (Fig. 6d). These coats appear as thin brown rims around the grains (Fig. 5b). These coats underlie quartz overgrowths (Fig. 6a) and carbonate cement suggesting they formed early in the sequence of mineral growth. The brown rims have variable present-day mineralogy and can include chlorite (Fig. 6a) and both illite and smectite.

Pyrite framboids are present especially in the Badenian sample at 1751 m (Fig. 6c). Framboids are broadly typical of bacterial sulphate reduction and thus seem to confirm marine sedimentary environments in the Badenian (Sauer et al., 1992).

Glauconite, broadly assumed to be an indicator of deposition in shallow marine sedimentary conditions (e.g. Odin and Matter, 1981), is present in almost all the samples. Fig. 5a shows glauconite grains in Karpatian sandstone although these rocks were not deposited in a marine environment (Sauer et al., 1992), instead being deposited in lacustrine and fluvial environments. This anomaly suggests that some glauconite in these Neogene sandstone is probably reworked allochthonous grains rather than authigenic cements (Amorosi, 1995).

Grain contacts are dominated by long and concavo-convex surfaces that have likely resulted from compaction. Clay coats sit between some grain-to-grain surfaces suggesting the grain-coating clay developed before mechanical compaction started (Fig. 5). Mica grains have been deformed and bent around more rigid grains and delicate grains of bioclastic debris have been extensively brittly deformed.

Feldspar grains, especially detrital K-feldspars, contain significant secondary porosity that must have developed during burial and diagenesis (Fig. 5b, c). In some cases, the secondary porosity has been partially occluded by kaolin while other cases have minor carbonate cement growth within secondary pores in feldspars.

At depths greater than ~1500 m, very small quantities of euhedral quartz overgrowths are evident in thin sections and SEM (Fig. 6a, b, d, f). It is not easy to discriminate quartz overgrowth from detrital grains in thin section (Fig. 5c) although it is evident that these seem to be fairly anomalous sandstones since even the deepest, hottest samples have relatively little quartz cement. Quartz cement represents no more than ~1% of the whole rock. Grain-coating clay (e.g. chlorite, Fig. 6a; but including illite and smectite) has been overgrown by diagenetic quartz. In some cases, small quartz crystals seem to have grown over the chlorite coat suggesting that the coat is not very well developed.

The total carbonate content, including bioclastic debris, limestone rock fragments and cement, is relatively widely variable with depth of burial and seems to show no simple pattern (Fig. 7) implying that the amount of carbonate (cement) is not a function of degree of diagenesis or material flux. Carbonate cement (Fig. 6e, f) occurs in two different forms. One type is a rather patchy, local cementation (Fig. 5d), where calcite grains have been dissolved and reprecipitated around other detrital grains. It proved not feasible to uniquely identify whether a patch of calcite was a deformed detrital grain (Fig. 5a) or pore-filling cement (Fig. 5d). Indeed, it is likely that even discernibly detrital components have dissolved and recrystallised since all carbonate entities stain a very uniform dark mauve characteristic of ferroan calcite. The other type of calcite is

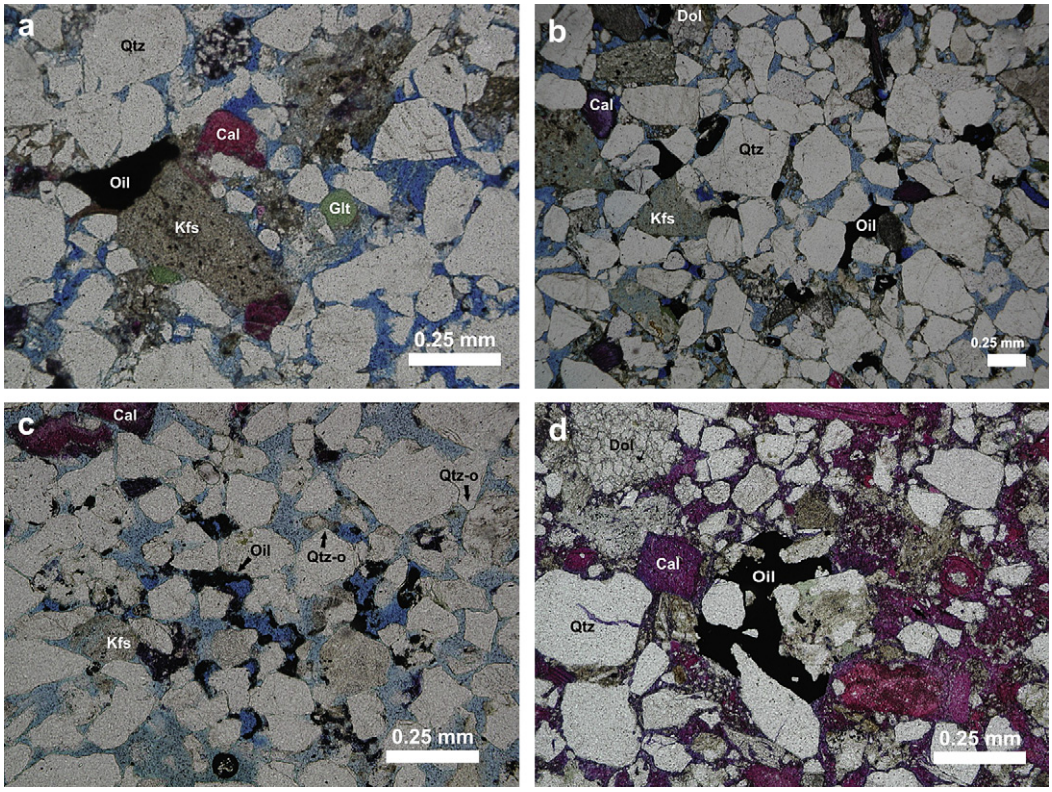

Fig. 5. Thin section images of sandstones (pore space is shown in blue, calcite particles have been stained red): (a) Sample 2353 m: quartz and glauconite grains, partially dissolved K-feldspar and calcite grains. Clay mineral cement and oil staining are present. (b) Sample 2068.5 m: quartz, dolomite and calcite grains and secondary porosity in detrital K-feldspar. Thin brown clay-coatings occur around grains and there is oil staining. (c) Sample 1683 m: diagenetic sequence revealed to be K-feldspar dissolution, quartz overgrowths, neo-formation of clay minerals, oil migration. (d) Sample 2774 m: diagenetic sequence revealed to be K-feldspar dissolution, quartz overgrowths, neo-formation of clay minerals, significant occlusion of porosity by calcite cement and oil migration. Key – detrital grains: quartz (Qtz), glauconite (Glt), K-feldspar (Kfs), calcite (Cal), dolomite (Dol); cement: quartz overgrowth (Qtz-o).

where there has been complete cementation of the sandstones (e.g. Figs. 5d, 7). At these locations, the ferroan calcite includes initial grains and all pores now filled with cement. This explains how the total quantity of carbonate can be considerably in excess of 45% typical of pre-compactional porosity values (Fig. 7). Secondary X-ray analysis of carbonate grains and cement during electron microprobe examination shows that they have a very homogenous chemical composition and are relatively pure calcite with a minor but significant iron presence.

A kaolin-type mineral sits in primary pores as well as within secondary pores in feldspar grains. Kaolin mainly is present as euhedral kaolin booklets filling primary porosity within the sandstone (Fig. 5a, c). Kaolin occurs as stacks of pseudohexagonal plates or books. SEM examination revealed that kaolin crystals overlie both calcite and quartz cements (Fig. 6b, f), leading to the conclusion that kaolin was one of the latest diagenetic minerals to form in the sandstones.

4.3. Clay mineralogy variation with depth

Clay minerals in the $<2\,\mu m$ fractions of sandstone samples consist of mixed layer illite/smectite (I/S), illite, a kaolin mineral and chlorite (Fig. 9).

XRD spectra confirm the petrographic identification of a kaolin mineral (Fig. 9) and show that it is variably present throughout the whole Neogene succession. XRD cannot easily discriminate different kaolin polymorphs but FT-IR spectra revealed that kaolinite ($\sim$7 Å polymorph) is present throughout the entire section: there is no dickite (the $\sim$14 Å polymorph) present even in the deepest samples (Fig. 8a). The intensity of kaolinite 001 reflections (XRD data) show the greatest abundance of kaolinite over the depth range 2100–2500 m (Karpatian section). Using FT-IR spectra, reference to the calibrated standards of pure kaolinite allowed quantification of the amounts of kaolinite in the $<2\,\mu m$ fractions. The data reveal that there is no systematic variation of the quantity of kaolinite with depth but the $<2\,\mu m$ fractions of some samples between 2100 m and 2500 m have between 25% and 50% kaolinite (Fig. 8d).

FT-IR data do not seem to be particularly useful for discerning the relative proportions of smectite and illite in clay fractions since they both have dominant bands at about 3620 cm^{-1} (De la Fuente et al., 2000). However, the sum total of I/S minerals can be quantified using FT-IR absorbance data. The interpreted I/S FT-IR data hint at a trend of increasing total quantity of the sum total of I/S minerals with increasing depth (Fig. 8b).

XRD must be used to discriminate smectite from illite. XRD data from the $<2\,\mu m$ fraction from the shallowest sandstone sample (892 m) contains 24% illite in I/S and is randomly interstratified ($R = 0$) (Fig. 9a). In the XRD traces of the $<2\,\mu m$ fractions, illitisation of the I/S mixed layer mineral occurs progressively with increasing depth. The percentage variation of the illite component in the I/S phase as a function of depth is shown in Fig. 10. The sample from 1699 m contains about 51% illite in I/S and shows evidence of ordered I/S in coexistence with the randomly interstratified I/S. The ordering is seen by a weak reflection at around 27 Å, which is the (001) trace of the superstructure reflection. Illitisation increases to a maximum of about 84% illite layers in this Neogene sedimentary succession. I/S consistently has R1 ordering at all depths greater than $\sim$2000 m. A deep sample (2353 m) shows R1 I/S ordering and incidentally a prominent kaolinite peak (Fig. 9a).

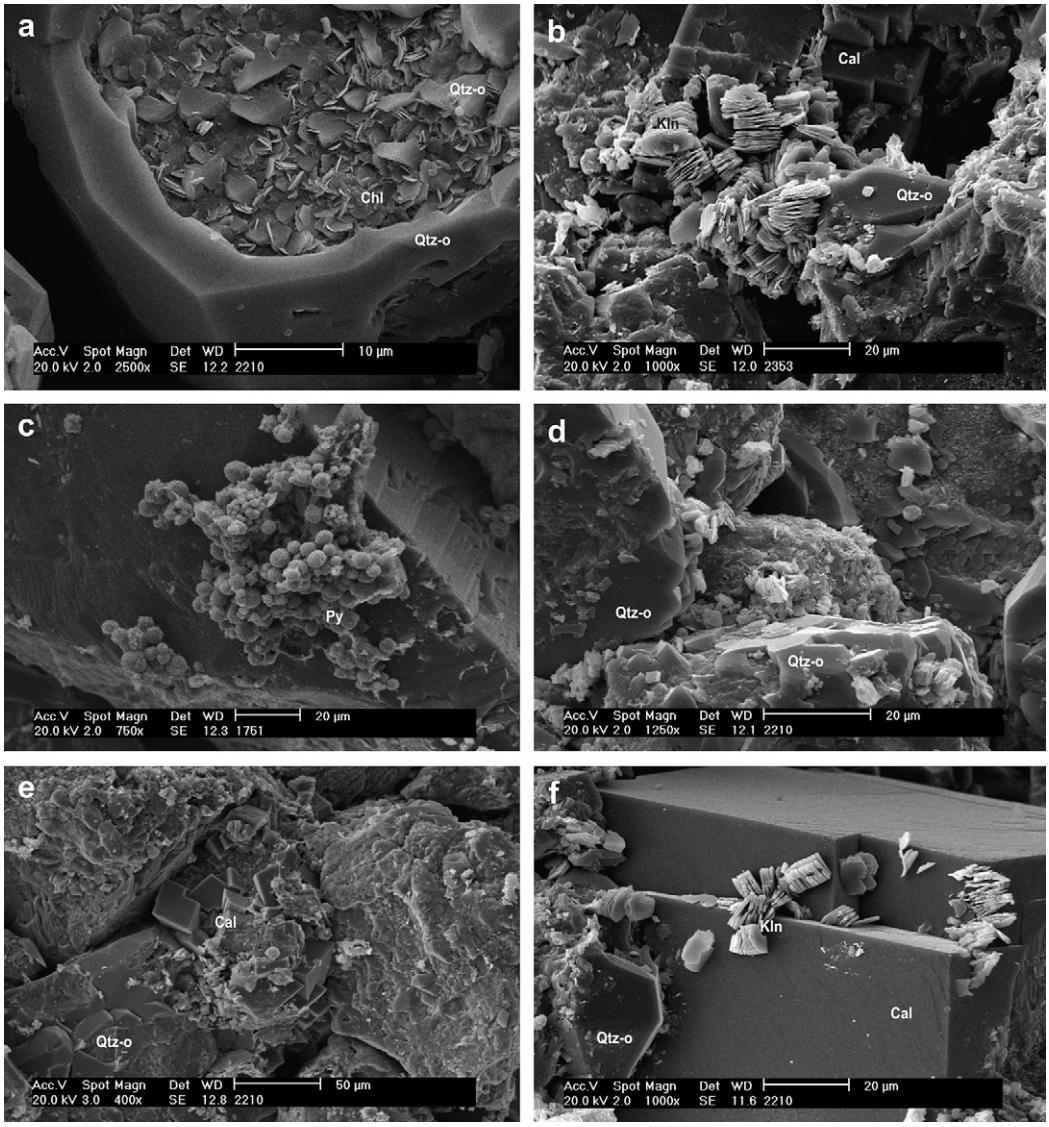

Fig. 6. SEM images of sandstones. (a) Sample 2210 m: chlorite coat on a detrital quartz grain, overgrown by euhedral quartz cement. (b) Sample 2353 m: well crystallized, authigenic kaolinite, overgrowing calcite and quartz cements and partly filling pores. (c) Sample 1751 m: pyrite framboids growing on a detrital K-Feldspar grain. (d) Sample 2210 m: clay-coated detrital grain (centre) surrounded by quartz grains with incipient quartz cementation. (e) Sample 2210 m: calcite cement blocking pore throats, quartz cementation occurred before calcite growth. (f) 2210 m: quartz cement engulfed by calcite cement, well-crystallized kaolinite booklets overlying both calcite and quartz cements. Key: chlorite-coats (chl), quartz overgrowth (Qtz-o), kaolinite (Kln), calcite cement (Cal), pyrite cement (Py).

The occurrence of chlorite, petrographically determined to be a minor cement, is confirmed by XRD and SEM data from some of the more porous sandstones in the stratigraphy (Fig. 9 and Fig. 6a).

4.4. Oil presence in the Miocene section

Based on the petroleum production history and thin section evidence (bitumen staining) oil was definitely present in a number of samples in the middle part of the Badenian section (1670–1700 m). There is also thin section evidence of oil (bitumen staining) at the base of the succession (2625 m, 2774 m) in the Karpatian.

Infrared spectroscopy can be used to detect organic materials as well as minerals; alkane linkages ($-CH_2$ and $-CH_3$) can be found at about 2927 cm^{-1} (Fig. 11a). The total areas of the bands produced by alkane bonds for all <2 µm fractions were derived using OMNIC and have been plotted as a function of depth (Fig. 11b). This illustrates minor hydrocarbons are present in all samples but there is a notable concentration at about 1700 m confirming the petrographic observation about oil staining.

The reservoir sandstones of the Miocene (Badenian) succession (locally oil-stained in thin section) do not seem to display any systematic variations in diagenesis in comparison to sandstones without oil staining. They neither have more nor less carbonate or quartz cement and do not have different clay mineral populations.

4.5. Porosity variation with depth

In general, the Miocene sandstones in the Vienna basin contain relatively high primary interparticle porosity. The maximum porosity value for any given depth range tends to decrease with increasing depth. Maximum porosity values are greater than ~30% at 1000 m but are less than ~15% at 2700 m (Fig. 12). The oil-bearing sandstones, occurring in the depth-interval 167–01753 m, have porosities ranging from 17% to 26%.

Secondary intragranular microporosity, resulting from feldspar dissolution (Fig. 5b, c), is present in these rocks but is relatively

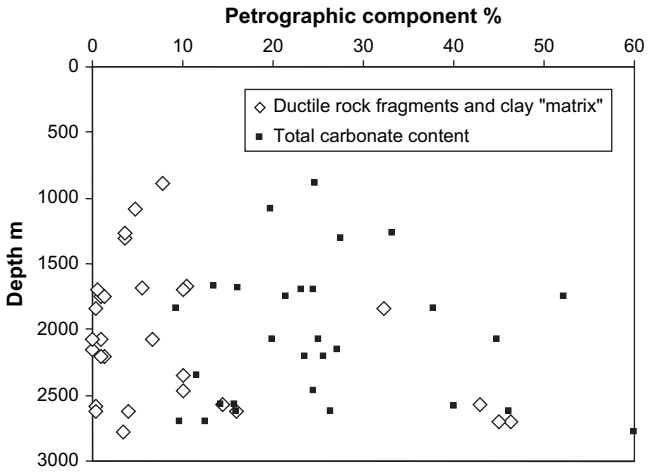

Fig. 7. Variation of carbonate and clay-rich detrital materials versus depth. Carbonate here includes detrital grains, bioclastic fragments and carbonate cement (mainly ferroan calcite). Grains here include detrital clay mineral-rich detrital rock fragments, clay matrix of uncertain (but probably detrital) origin, etc.

minor. Any secondary porosity after the dissolution of carbonate grains has not led to an increase in net porosity since the dissolved material will have, on the evidence of the quantity of carbonate cement (Fig. 7), been locally reprecipitated.

5. Discussion

5.1. Paragenetic sequence: order of cement growth and sources of cements

In summary, the dominant eogenetic features in the sandstones of the Aderklaa-78 well are the formation of thin authigenic clay-coatings around most of the detrital grains and the formation of pyrite framboids and possibly glauconite although this mineral maybe from reworked grains in some or most cases. Also in summary, subsequent mesogenetic changes experienced by these sandstones include compaction, partial dissolution of K-feldspars, development of minor euhedral quartz overgrowths, ferroan calcite cementation and illite, illite/smectite, pore-filling kaolinite and localized development of grain-coating chlorite. The relative timing was inferred from their textural relations as observed in thin section and in the SEM (Figs. 5 and 6). The interpretation of the relative timing of these events is presented in Fig. 13. Quartz cement was only found in samples deeper than about 1500 m. Ferroan calcite is the most important pore-occluding mineral. In shallower samples, there are abundant discernable detrital carbonate lithic fragments which are similar in size to detrital quartz and feldspar grains. These were presumably eroded from relatively proximal mountain belts (e.g. Northern Calcareous Alps). In deeper samples, it becomes increasingly difficult to discriminate ferroan calcite grain from

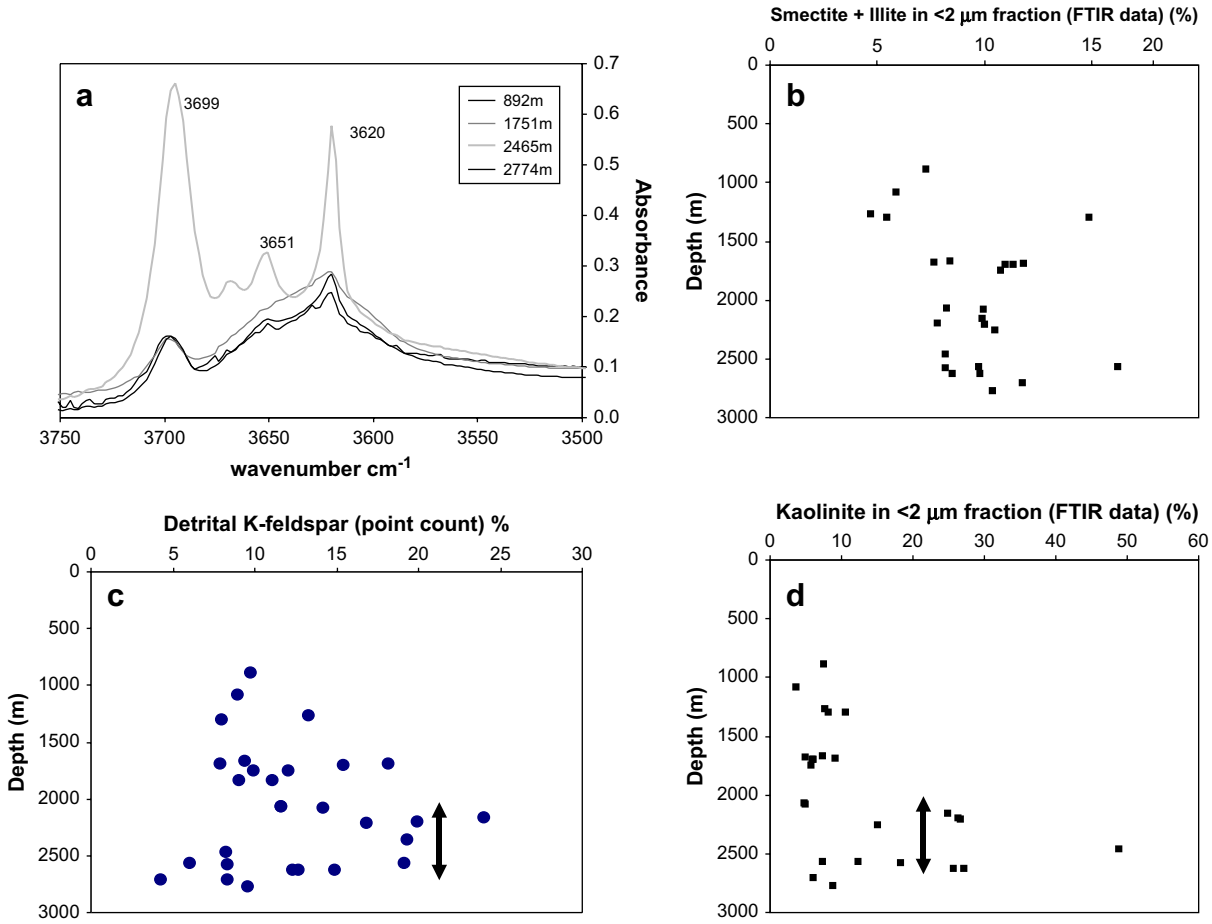

Fig. 8. Detrital feldspar abundance and data from the FT-IR clay-hydroxyl region of the spectrum with a variety of bands illustrated. The bands were deconvoluted and areas determined using OMNIC based on Gaussian peaks with a full width–half height ratio of ten. (a) The area of the 3699 band is only associated with kaolinite and was converted to quantity of kaolinite by reference to variably diluted pure kaolin standards. The area of the 3620 band resulting from I/S was determined by subtracting half the 3699 band area from the total 3620 band since this is contribution made by kaolinite. The area of the 3620 band was quantified by assuming that this band has the same response factor as the 3699 band. (b, c and d) The quantities of kaolinite and I/S are plotted as a function of depth and compared to the point-counted quantity of detrital K-feldspar.

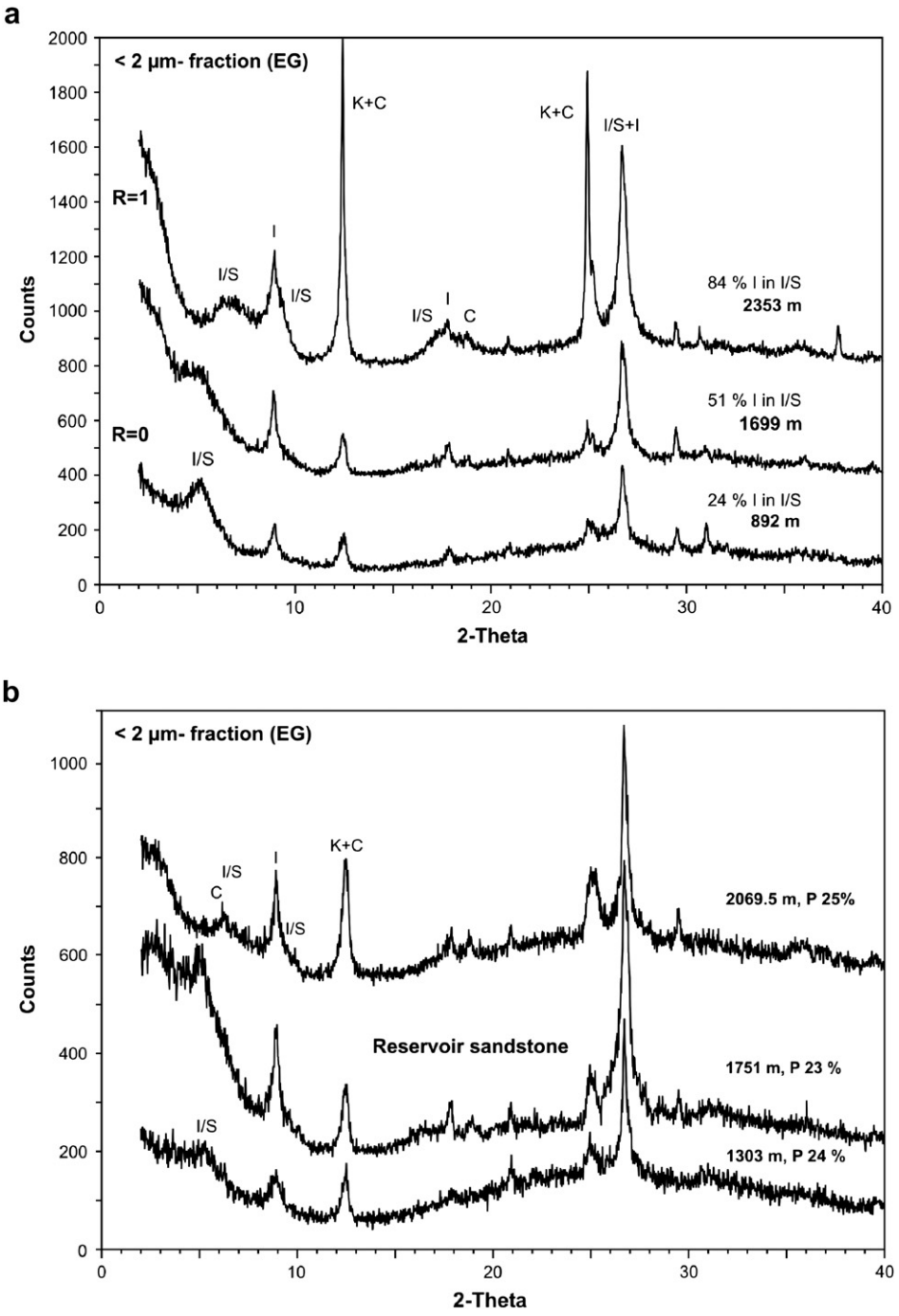

Fig. 9. XRD patterns. (a) Oriented, EG-saturated < 2 μm fraction samples from different depths. I/S, illite/smectite; I, illite; K, kaolinite; C, chlorite; R0, randomly interstratified; R1, ordered. (b) Oriented, EG-saturated < 2 μm fraction samples from a reservoir sandstone (1751 m) and non-reservoir sandstones (1303 m, 2069.5 m). I/S, illite/smectite; I, illite; K, kaolinite; C, chlorite.

ferroan calcite cement: the latter has seemingly grown on top of, and replaced, the former.

Oil was found in the sandstones of the Upper Lagenid Zone (samples from 1670 m to 1753 m depth). Fig. 5c shows a thin section of a core from 1683 m where the porosity is 26%, oil and asphaltic residues effectively fill pore space in sandstones. In this thin section there is clear oil staining along the rims of pores. The XRD pattern of the clay mineral fraction of this oil-stained sample is effectively identical to the XRD pattern from non-reservoir sandstones. There are no differences in terms of authigenic clay mineral fraction of the quantities of calcite or quartz cement.

5.2. Sources of mineral cements

The framboidal pyrite was almost certainly the result of bacterial sulphate reduction in marine environments with the sulphate supplied from the ambient seawater and the iron supplied by the localized reduction of detrital ferric detritus. According to previous interpretation from other systems, the clay coats reported here may have a range of origins including: inherited coats (Wilson, 1992) infiltrated clays (Moraes and De Ros, 1992), bioturbation (Wilson and Pittman, 1977) and the acts of sediment ingestion and excretion (Needham et al., 2004, 2005). At present there is no simple way of

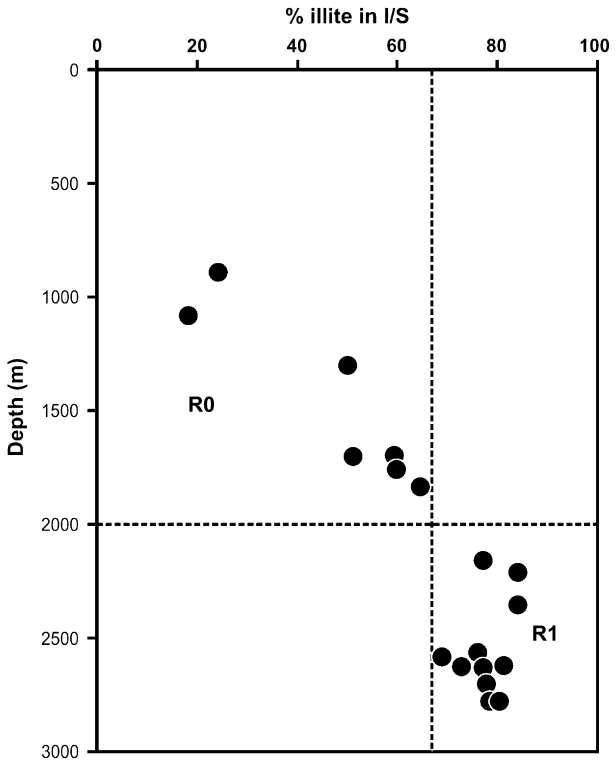

Fig. 10. The percentage of illite component in the interstratified illite–smectite (I/S) phase, plotted as a function of depth (R0, randomly interstratified I/S; R1, ordered I/S).

discriminating the origin of grain-coating clay especially given the great extent of compaction and localized extreme quantities of carbonate cement.

The carbonate cement will have been derived from dissolved and locally reprecipitated detrital carbonate grains, bioclasts, etc. The shallowest samples have the greatest quantity of discernible bioclasts but none are visible in the deepest samples. The fact that it stains mauve from the shallowest to the deepest sample testifies to the iron-rich nature of the carbonate and implies that even coherent bioclasts have dissolved and locally reprecipitated.

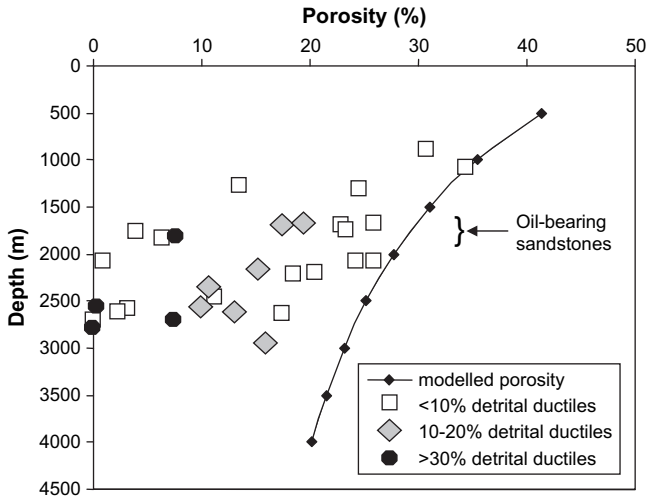

Fig. 12. Porosity-depth plot in comparison to global sandstone porosity-depth plot (from Gluyas and Cade, 1997). The highest porosity Tertiary sandstones in Aderklaa-78 conform to the compaction curve although many samples have lower porosity than would be expected from compactional processes alone.

Detrital K-feldspar grains have undergone partial dissolution (Fig. 5b, c). Simple observations of the abundance of detrital feldspar and the quantity of kaolinite suggest that the dissolved K-feldspar can easily have sourced the kaolinite and coincidentally facilitated the transformation of smectite into illite through the supply of potassium (Worden and Morad, 2003). There are no other obvious sources of Al for the kaolinite cement although it is not impossible that some was derived from reaction of detrital clay minerals. The illite found in the deeper of these sandstones will be the result of transformation of smectite as a function of temperature (see later). The smectite to illite transform, well known and documented in mudstones, is also important in sandstones (McKinley et al., 2003). The minor grain-coating chlorite found in deeper samples is also likely to be the result of transformation of detrital or eogenetic clay minerals.

The origin of quartz cement in sandstones has been controversial for a long time with fundamental arguments about external versus internal sources of silica within a given sandstone. Various internal sources of silica have been proposed including chemical

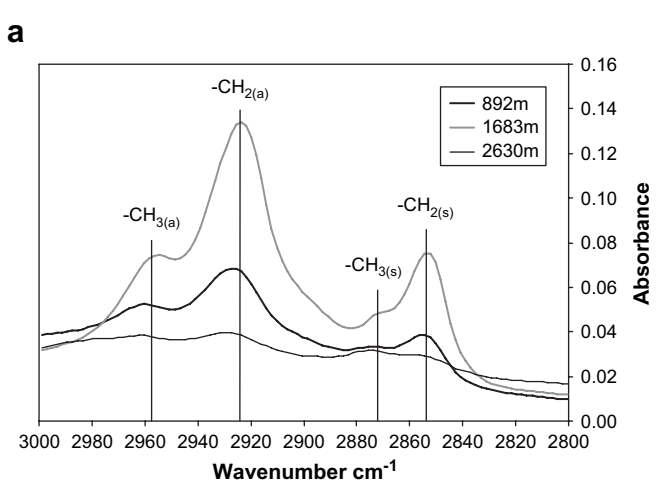

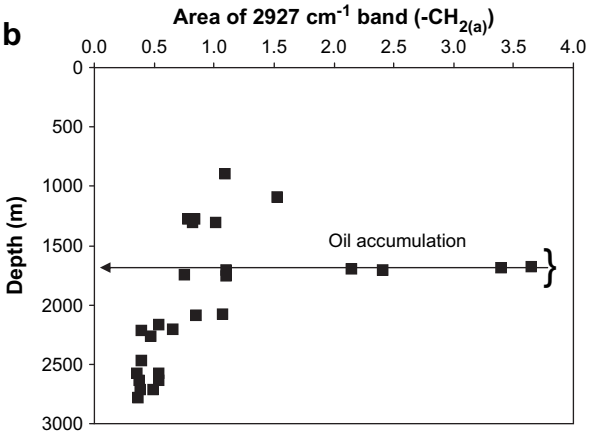

Fig. 11. Alkane spectra revealed by FT-IR analysis. (a) Typical spectra collected from <2 μm samples at the same 0.5 wt% concentration in KBr discs (transmission IR spectra). The vibrational peaks are labelled by moiety with subscript-s represent symmetric vibrations and subscript-a representing asymmetric vibrations. (b) Variation of area of the asymmetric $-CH_2$ band (proportional to quantity of oil) plotted as a function of depth revealing a spike coincident with the presence of oil staining in thin section.

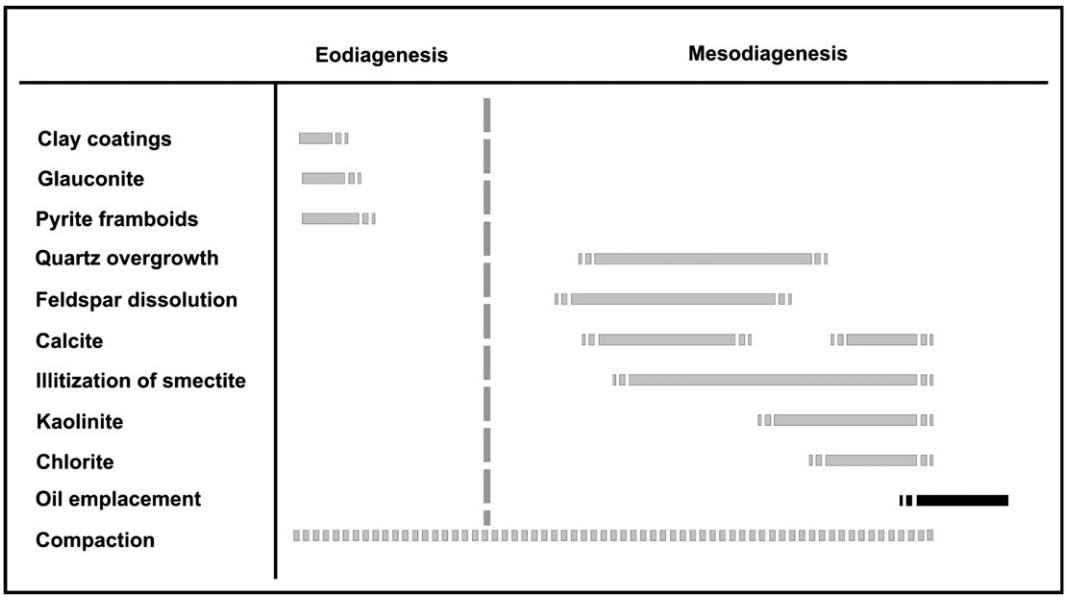

Fig. 13. Paragenetic sequence for the main diagenetic processes that occurred in the sandstones, as interpreted from petrographic relationships.

compaction (pressure solution, stylolites), reaction of smectite to illite, reaction of detrital feldspar minerals, etc. (Barclay and Worden, 2000; Worden and Morad, 2000). In these sandstones, the absence of quartz cement in the shallower samples and its appearance in the deeper samples suggests a significant depth, and possibly temperature, control on its development. It is possible that the quartz cement in these Neogene rocks has more than one source; it is likely that some silica has come from the reacted and partially dissolved K-feldspar grains. Some may also have derived from smectite during its progressive transformation to illite (McKinley et al., 2003). Pressure solution may have been important in these sandstones but there is no unequivocal evidence to support this notion.

In summary, the mineral cements in these sandstones can seemingly be explained by a series of reactions and processes that do not require mass flux (i.e. diagenesis may be more or less isochemical). There is no need to invoke fluid flow and movement of material in order to account for the various minerals and cements found in these Neogene sandstones. This is an important deduction since questions about reservoir quality for these rocks can presumably be explained by features intrinsic to the sandstones combined with burial and thermal histories.

5.3. Role of compaction on porosity

Porosity tends to decrease with increasing depth (Fig. 12) although simple mechanical compaction (rearrangement of grains) is not the only control on porosity since the depth-porosity variation is complex and varied. The maximum porosity value for a given depth-interval seems to correspond to modelled theoretical compaction curves (Gluyas and Cade, 1997). The spread of data relative to the compaction curve suggests that these sandstones have not been overpressured since this would lead to porosity values greater than that predicted by theoretical compaction curves (Osborne and Swarbrick, 1999). However, most samples have significantly lower porosity than the theoretical maximum values. This could be due to either cementation or ductile compaction or a combination of the two. Cement growth reduces the porosity since minerals grow in pore spaces. Ductile compaction occurs when some of the detrital grains undergo not just intergranular rearrangement but plastic deformation (Worden et al., 2000). Ductile grains tend to be clay mineral rich and can have a wide variety of origins from metapelites to mudstones and mud intraclasts. Plastic (as opposed to brittle) deformation tends to lead to smearing of ductile grains around more rigid (i.e. quartz) grains and efficiently reduce porosity during burial. Oil-stained samples do not seem to be unusual relative to the non-oil-stained samples since they also display a wide range of porosity values (Fig. 12). Oil emplacement does not seem to have changed porosity-loss patterns. Oil is sometimes implicated in porosity-preservation in sandstones (e.g. Worden et al., 1998; Yurkova, 1970) but here it seems to have had no influence.

5.4. Timing of oil generation in the depocenter and influence of petroleum emplacement on reservoir quality

The main source rock lies in the pre-Neogene autochthonous section. The timing of oil generation is uncertain for any individual part of the basin although it seems that generation occurs when source rocks are buried to 4000–6000 m (Ladwein, 1988). The Upper Jurassic source rocks experienced lower temperatures in the basin margins and so will have generated oil *later* than in the basin-centre. It is thus difficult to predict the timing of generation of oil found in the core (Figs. 5 and 11) and even harder to predict the timing of oil accumulation.

In the Aderklaa-78 profile, pore-filling kaolinite seems to have been the last mineral to form in the sandstones although it seems that smectite transformation to illite is also an ongoing, and therefore late-stage, process. This relatively late time of mineral growth allows these clay minerals (especially kaolinite and illite) to be used as indicators to compare the diagenesis of reservoir- and non-reservoir sandstones. For this comparison it is necessary to use reservoir- and non-reservoir sandstones of about the same initial porosity and framework composition.

Diffractograms of the $<2\ \mu m$ fractions of non-reservoir sandstones above (1303 m, porosity 24%) and below (2069.5 m, porosity 25%) the reservoir are shown in Fig. 9b. The trace plotted in the middle is the $<2\ \mu m$ fraction of a reservoir sandstone that originates from 1751 m (porosity 23%). As can be seen in this figure, the clay mineralogy of this reservoir sandstone is quite similar to the non-reservoir sandstones, excluding any depth-dependent changes

of the clay minerals. This is true for all the reservoir sandstones and, assuming that the addition of oil inhibits diagenetic processes (e.g. Worden et al., 1998; Worden and Morad, 2000), suggesting that the oil must have migrated into the sandstone as a late diagenetic event after the diagenetic growth of pore-filling kaolinite, illite (in I/S) and even chlorite. It thus seems likely that the late addition of oil to the Badenian sandstones at about 1700 m was either much delayed relative to oil generation in the local source kitchen or was derived from more distant basin settings (Ladwein, 1988 and see previous).

5.5. Thermal history of the Miocene sandstones (1): modelling of illite/smectite (I/S) data and calibration of thermal histories

The I/S data reveal a steady increase in the proportion of illite with increasing depth (Fig. 10). The transformation of smectite into illite is a kinetically controlled process that is a function of number of factors: time–temperature history, kinetic constants (activation energy, frequency factor) and the initial illite fraction in the I/S (e.g. Wei et al., 1996). In a well with a continuous cored section such as Aderklaa-78, it is possible to fit a modelled curve to the I/S data using a range of kinetic constants and a variety of reasonable thermal histories of all significant geological boundaries (formation bases and/or tops of known age in millions of years). Modern approaches to understanding I/S transformation kinetics have evolved to accommodate the notion that smectite, even in one sedimentary succession, is not a single mineralogical entity but likely has a range of mineral chemistries each of which may have its own set of kinetic constants (e.g. Wei et al., 1996). This is practically accommodated by choosing a range of activation energies and assigning a probability distribution to each value in this range. Wei et al. (1996) usefully illustrated the I/S curve shapes of a range of frequency distributions.

The data from Aderklaa-78 resemble a bimodal distribution of I/S activation energies. A suite of burial curves for the significant geological boundaries were then converted into temperature assuming a given geothermal gradient (initially 30 °C/km, as described earlier; after Sachsenhofer, 2001). A range of activation energy distributions was then tested to reproduce the shape of the actual I/S-depth pattern. The frequency factor was then varied to best match the maximum and minimum I/S values for the shallowest and deepest samples. A series of iterations followed including alteration of the heat flow, the frequency factor and the spread of activation energies. The fitted curve in Fig. 14b uses the frequency distribution illustrated in Fig. 14a and represents the best fit achieved in this exercise. A heat flow of 30 °C/km seems to be a reasonable estimate for the Miocene and afterwards.

The implication of the bimodal I/S kinetics (Fig. 14a) is that there are two sorts of smectite in the Aderklaa-78 Miocene sediments, presumably differentiated by mineral composition, crystal structure, or both. The XRD data seem to corroborate this model since the XRD data reveal two types of smectite (ordered and disordered, Fig. 9). These likely have discrete primary sources in the sediment's hinterland. The thermal histories for each significant geological boundary can now be used to help understand other diagenetic phenomena in the sediments.

5.6. Thermal history of the Miocene sandstones (2): simulation of quartz cementation

Quartz cementation, like most diagenetic phenomena, is a kinetically controlled process. There is widespread controversy about whether quartz grows in short, fast bursts (episodic) or in a long, continuous but, inevitably slow, manner (Worden and Morad, 2000). While we are not taking sides in this debate here it is certain that quartz is more abundant in deeper sandstones in some basins (e.g. Giles et al., 2000) and it is notoriously difficult to *model*

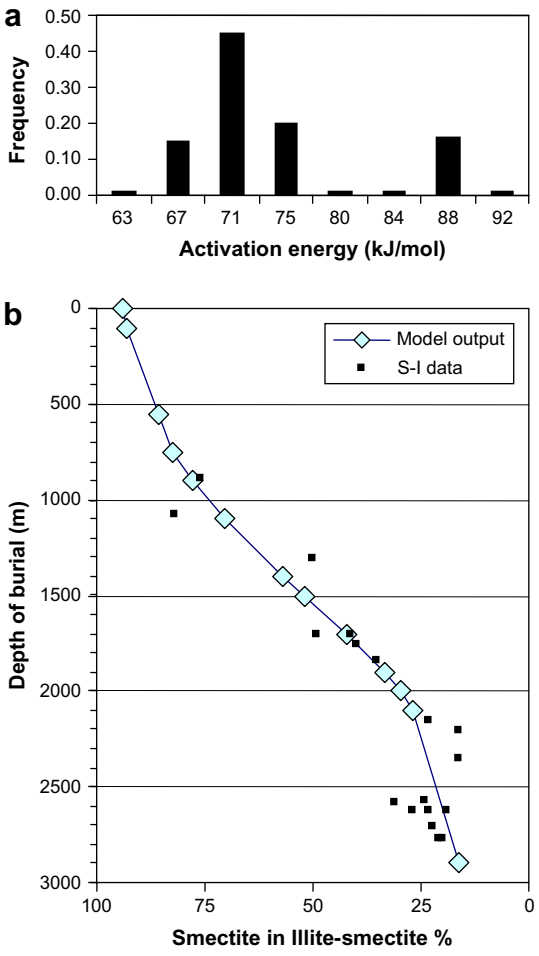

Fig. 14. Model of smectite to illite conversion in comparison to clay mineral data from Tertiary sandstones in the Vienna Basin. The model was developed using an initial smectite–illite ratio of 95%, a frequency factor of 0.0008 s^{-1} and the spread of activation energies as shown in (a). The model employs a range of activation energies following Wei et al. (1996) predicated upon the concept that "smectite" is a mixture of minerals rather than a pure and uniform mineral. The burial history was synthesised using the thicknesses of units shown in Fig. 2 and the ages of the units reported in Wagreich and Schmid (2002). The model was optimised to best fit the data by systematically varying the frequency factor to cover the range of smectite–illite ratios over the depth-interval and then altering the distribution of activation energies to simulate the shape of the smectite–illite transformation as a function of depth. The current geothermal gradient of 30 °C/km was initially employed (Sachsenhofer, 2001). It proved unnecessary to vary this to successfully reproduce the shape of the smectite–illite transformation data.

the growth of short, fast bursts of quartz growth. We here have used the empirically derived quartz kinetic growth model of Walderhaug (1994) and Walderhaug et al. (2000), calibrated from North Sea sandstones, as a means of trying to understand why there is so little quartz cement in the sandstones from Aderklaa-78. The modelling approach (Walderhaug et al., 2000) ignores the effects of fluid pressure and effective stress (Sheldon et al., 2003) and has been used to contend that petroleum emplacement has no influence on mineral processes in sandstone reservoirs (Worden and Morad, 2000). However, the model is capable of incorporating the combined influences of time and temperature and is a suitable tool to try to understand quartz cementation patterns in these Miocene sandstones.

We have assumed a grain size of 150 μm, that 60% of the detrital grains are quartz (and thus available to grow syntaxial cement; Fig. 4) and that 40% of quartz grains are coated with minerals (predominantly clays) that prevent direct quartz cement growth. To develop the argument, we have taken kinetic

constants directly from Walderhaug (1994) and two thermal histories (calibrated to the illite/smectite data, Fig. 14); one from the base of the Miocene section and one from the Badenian interval that is liberally stained with oil (the nominal reservoir, Figs. 2, 5 and 12). The I/S modelling-derived thermal history curves are displayed in Fig. 15a. The resulting models of quartz cement growth (Fig. 15b) illustrate why so little quartz cement is found in the shallower more porous parts of the section, including the reservoir. Quite simply, the rocks have never been hot enough for a long enough period of time. However, it seems that more quartz cement should theoretically be found in the deepest parts of the Miocene although these samples mostly have low porosity (Fig. 12). Large quantities of pore-occluding ferroan calcite cement seem to have prevented quartz from growing in some of these samples.

The lack of quartz cement can thus be neatly explained by a combination of the rocks being too young (insufficient time) and the geothermal gradient being too low (too cool). On top of this, some of the deepest samples that theoretically might have been able to develop significant volumes of quartz cement are almost totally cemented by ferroan calcite which seems to have prevented quartz cement from growing.

5.7. Roles of lithology-dependent compaction and carbonate cementation

Quartz cement, the most important cement in most sandstones, is here not an important control on reservoir quality. The question thus remains as to what controls porosity. The two main candidates revealed by the petrographic data are the presence of ductile detrital grains and the presence of carbonate cement. The petrographically determined quantities of ductile grains and carbonate cement have been plotted against porosity and both display a triangular spread of data suggesting that both parameters exert a significant control on porosity (Fig. 16). The graph of carbonate content versus porosity has been split as a function of the quantity of ductile lithic grains (Fig. 16a). Similarly, the graph of ductile lithic grains versus porosity has been split as a function of the amount carbonate content (Fig. 16b). These graphs unequivocally illustrate that both carbonate content and ductile lithic grain content are important controls on porosity. The porosity data plotted as a function of depth (Fig. 12) have been subdivided by the quantity of ductile lithic grains to help illustrate the paramount importance of

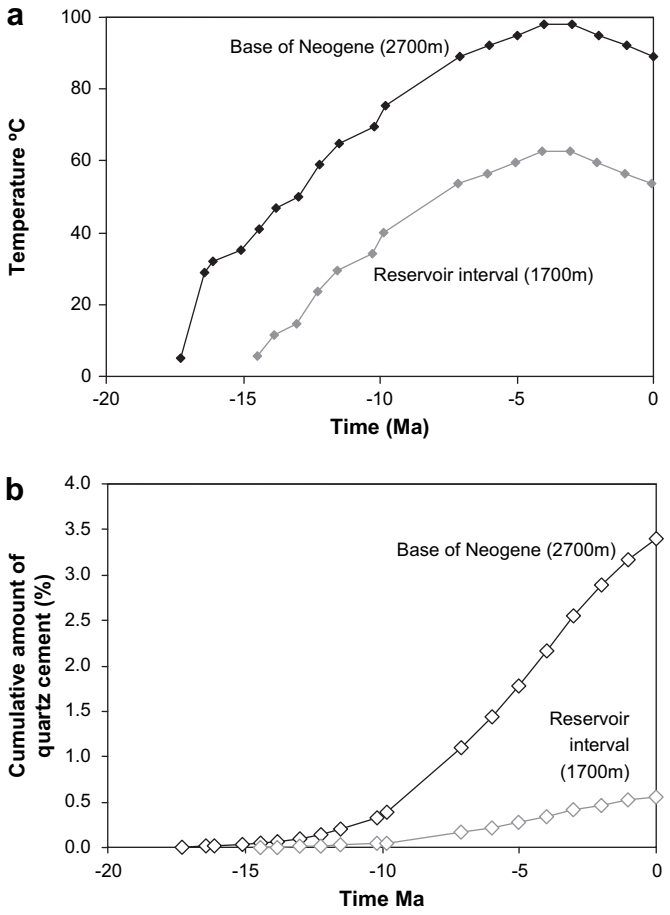

Fig. 15. Model of quartz cementation for the Tertiary sandstones of the Vienna Basin, assuming 60% of the detrital grains are quartz, 40% of grains coated with clay and a grain size of 0.15 mm. Kinetic inputs have been taken from Walderhaug (1994) and Walderhaug et al. (2000). The thermal histories in part (a) have been calibrated from the T-t history fitted to the smectite–illite transformation model (Fig. 14), (b) shows the growth of quartz cement as a function of time in the Miocene section. One curve represents sandstones at the base of the Tertiary sedimentary section (~2700 m) while the other represents the shallower and younger sandstones of the reservoir interval ~1700 m (see Fig. 2). Even the deepest cleanest sandstones at the base of the Miocene section should have no more than 3.5% quartz cement due to the limited time and temperature experienced by these Tertiary sandstones. The oil field samples (~1700 m) should have negligible quartz cement (<0.6%) according to this approach.

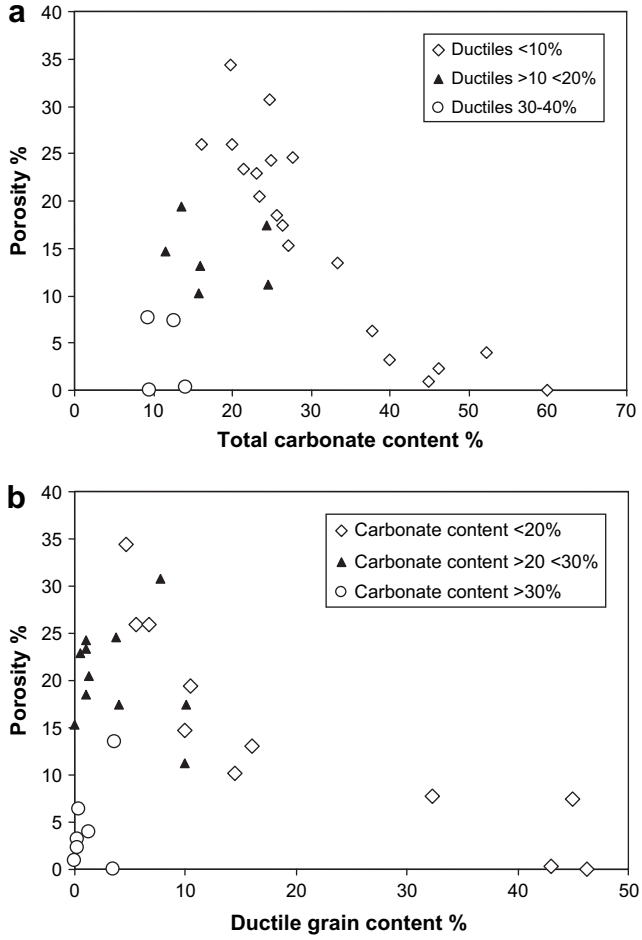

Fig. 16. Plot of the total amount of key reservoir quality controls as a function of porosity. (a) Total carbonate in the sandstone samples from Aderklaa-78 versus petrographically determined porosity split by the quantity of ductile (clay-rich) grains and matrix. Carbonate includes detrital grains, bioclastic fragments and carbonate cement (mainly ferroan calcite). (b) Total ductile lithic fragment from Aderklaa-78 versus petrographically determined porosity split by the quantity of total carbonate content. Ductile grains here include detrital clay mineral-rich detrital rock fragments, clay matrix of uncertain (but probably detrital) origin.

the nature of the detrital grains. The low porosity yet low ductile grain samples on Fig. 12 have high quantities of carbonate confirming that this is of great importance.

The quantity of ductile lithic grains is a function of the primary composition and mineralogy of the sediment (Worden et al., 2000). Similarly, the amount of carbonate is likely to be a function of the primary quantity of detrital carbonate rock fragments (and possibly first cycle bioclastic debris). While burial to depths of up to 2774 m and temperatures approaching 100 °C at the base of the section has led to compaction and dissolution and redistribution of carbonate grains as carbonate cement, a fundamental control on porosity was the primary composition of the sediment. There seems to be, at best, a limited role for material flux, oil-inhibition of diagenesis or even silicate dissolution and reprecipitation processes.

6. Conclusions

(1) The Miocene sediments in well Aderklaa-78 have porosity values varying from excellent (30%) to very poor (5%).
(2) The maximum porosity seems to broadly decrease with increasing depth of burial due to compactional processes. Ductile grain compaction has helped destroy porosity in sandstones where the initial ductile grain content was >10%. The highest porosity values for any given depth-interval approximately correspond to simple modelled compaction curve showing there was unlikely to have been significant overpressure.
(3) The Miocene sediments have decreasing smectite–illite ratios with increasing depth that have been successfully modelled using a bimodal spread of activation energies, a constant geothermal gradient for the Miocene and Pliocene and a series of thermal histories for dated geological surfaces. The bimodal frequency distribution of activation energies is probably a result of two discrete types of smectite present in these sandstones.
(4) Ferroan calcite cement is a major control on porosity being sourced from the dissolution of detrital limestone rock fragments.
(5) Models of quartz cement, representing less than 1% of the rock even at depth, have been based on the illite/smectite-calibrated thermal histories. These models have explained why quartz cement is not an important control on porosity; the rocks have not been to sufficiently high temperatures for long enough time. In the deepest part of the section, where a few percent of quartz cement could be anticipated, the rocks are too cemented with ferroan calcite.
(6) Porosity is only high in rocks that had a primary grain population that was poor in both carbonate grains and ductile lithic grains and commensurately was rich in quartz grains. Oil emplacement was a relatively late process and has had no role to play in porosity-preservation even though local oil generation occurred very soon after sediment deposition.
(7) The best reservoir quality must be sought in the cleanest sandstones with the smallest amount of carbonate cement and the lowest ductile grain content.

Acknowledgements

The authors thank OMV AG for providing the core samples of the well Aderklaa-78 and also for the license to publish this work. S. Gier acknowledges the financial support of the "Hochschuljubiläumsstiftung der Stadt Wien (Project H-166/2001)". We thank J. Weber (Universität für Angewandte Kunst Wien) and L. Ross (University of Missouri) for their assistance with the SEM. We also would like to thank E. Draganits for improving the figures. Furthermore, we thank editor Dave Roberts for his support and encouragement and two anonymous reviewers for their enthusiastic commentaries.

References

Amorosi, A., 1995. Glaucony and sequence stratigraphy: a conceptual framework of distribution in siliciclastic sequences. Journal of Sedimentary Research B65, 419–425.
Barclay, S.A., Worden, R.H., 2000. Geochemical modelling of diagenetic reactions in an arkosic sandstone. Clay Minerals 35, 61–71.
Burley, S.D., 1984. Patterns of diagenesis in the Sherwood Sandstone Group (Triassic), United Kingdom. Clay Minerals 19, 403–404.
De la Fuente, S., Cuadros, J., Linares, J., 2000. Quantification of mixed-layer illite-smectite in glass matrices by Fourier-transform infrared spectroscopy. Clay Clay Mineral 48, 299–303.
De Souza, R.S., De Assis Silva, C.M., 1998. Origin and timing of carbonate cementation of the Namorado sandstone (Cretaceous), Albacora Field, Brazil: implications for oil recovery. In: Morad, S. (Ed.), Carbonate Cementation in Sandstones. International Association of Sedimentologists Special Publication 26. Blackwell Science, pp. 309–325.
Ehrenberg, S.N., Jakobsen, K.G., 2001. Plagioclase dissolution related to biodegradation of oil in Brent Group sandstones (Middle Jurassic) of Gullfaks Field, northern North Sea. Sedimentology 48, 703–721.
Folk, R.L., 1968. Petrology of Sedimentary Rocks. Hemphills.
Giles, M.R., Indrelid, S.L., Beynon, G.V., Amthor, J., 2000. The origins of large-scale quartz cementation: evidence from large data sets and coupled heat-fluid mass transport modelling. In: Worden, R.H., Morad, S. (Eds.), Quartz Cementation in Sandstones. International Association of Sedimentologists Special Publication 29. Blackwell Science, pp. 21–38.
Gluyas, J., Cade, C.A., 1997. Prediction of porosity in compacted sands. In: Reservoir Quality Prediction in Sandstones and Carbonates. AAPG Memoir, vol. 69, pp. 19–28.
Hamilton, W., Wagner, L., Wessely, G., 1999. Oil and gas in Austria. Mitteilungen der Österreichischen Geologischen Gesell 92, 235–262.
Haszeldine, R.S., Macaulay, C.I., Marchand, A., et al., 2000. Sandstone cementation and fluids in hydrocarbon basins. J. Geochem. Res. 69, 195–200.
Horton, R.B., Johns, W.D., Kurzweil, H., 1985. Illite diagenesis in the Vienna Basin, Austria. Tschermaks Mineralogische und Petrographische Mitteilungen 34, 239–260.
Johns, W.D., Kurzweil, H., 1979. Quantitative estimation of illite–smectite mixed phases formed during burial diagenesis. Tschermaks Mineralogische und Petrographische Mitteilungen 26, 203–215.
Kurzweil, H., Johns, W.D., 1981. Diagenesis of tertiary marlstones in the Vienna Basin. Tschermaks Mineralogische und Petrographische Mitteilungen 29, 103–125.
Ladwein, H.W., 1988. Organic geochemistry of Vienna Basin: model for hydrocarbon generation in overthrust belts. AAPG Bulletin 72 (5), 586–599.
McKinley, J.M., Worden, R.H., Ruffell, A.H., Worden, R.H., Morad, S., 2003. Smectite in sandstones: a review of the controls on occurrence and behaviour during diagenesis. In: Clay Mineral Cement in Sandstones. International Association of Sedimentologists, Special Publication, vol. 34, pp. 109–128.
Morad, S., Ketzer, J.M., DeRos, L.F., 2000. Spatial and temporal distribution of diagenetic alterations in siliciclastic rocks: implications for mass transfer in sedimentary basins. Sedimentology 46, 95–120.
Moore, D.M., Reynolds Jr., R.C., 1997. X-ray Diffraction and the Identification and Analysis of Clay Minerals. Oxford University Press.
Moraes, M.A.S., De Ros, L.F., 1992. Depositional, infiltrated and authigenic clays in fluvial sandstones of the Jurassic Sergi Formation, Recôncavo Basin, Northeastern Brazil. In: Houseknecht, D.W., Pittman, E.D., Keller, W.D.F. (Eds.), Origin, Diagenesis, and Petrophysics of Clay Minerals in Sandstones: SEPM, Special Publication, vol. 47, pp. 197–208.
Needham, S.J., Worden, R.H., McIlroy, D., 2004. Animal-sediment interactions: the effect of ingestion and excretion by worms on mineralogy. Biogeosciences 1, 113–121.
Needham, S.J., Worden, R.H., McIlroy, D., 2005. Experimental production of clay rims by macrobiotic sediment ingestion and excretion processes. Journal of Sedimentary Research 75, 1028–1037.
Odin, G.S., Matter, A., 1981. De glauconiarum origine. Sedimentology 28, 611–641.
Osborne, M., Swarbrick, R.E., 1999. Diagenesis in North Sea HPHT reservoirs – consequences for porosity and overpressure prediction. Marine and Petroleum Geology 16, 337–353.
Sachsenhofer, R.F., 2001. Syn- and post-collisional heat flow in the Cenozoic Eastern Alps. International Journal of Earth Sciences 90, 579–592.
Sauer, R., Seifert, P., Wessely, G., 1992. Guidebook to excursions in the Vienna Basin and the adjacent Alpine-Carpathian thrustbelt in Austria. Mitteilungen der Österreichischen Geologischen Gesell 85, 1–264.
Selley, R.C., 1997. Elements of Petroleum Geology. Academic Press.
Sheldon, H., Wheeler, J., Worden, R.H., Lind, A., Cheadle, M.J., 2003. An analysis of the roles of stress, temperature, and pH in chemical compaction of sandstones. Journal of Sedimentary Research 73, 64–71.
Wagreich, M., Schmid, H.P., 2002. Backstripping dip-slip fault histories: apparent slip rates for the Miocene of the Vienna Basin. Terra Nova 14, 163–168.
Walderhaug, O., 1994. Precipitation rates for quartz cement in sandstones determined by fluid inclusion microthermometry and temperature-history modelling. Journal of Sedimentary Research 64, 324–333.

Walderhaug, O., Lander, R.H., Bjørkum, P.A., Oelkers, E.H., Bjørlykke, K., Nadeau, P.H., 2000. Modelling quartz cementation and porosoity in reservoir sandtones: examples from the Norwegian continental shelf. In: Worden, R.H., Morad, S. (Eds.), Quartz Cementation in Sandstones. International Association of Sedimentologists Special Publication, vol. 29. Blackwell Science, pp. 39–49.

Wei, H., Roaldset, E., Bjorøy, M., 1996. Parallel reaction kinetics of smectite to illite conversion. Clay Minerals 31, 365–376.

Wilson, M.D., Pittman, E.D., 1977. Authigenic clays in sandstones: recognition and influence on reservoir properties and paleoenvironmental analysis. Journal of Sedimentary Petrology 47, 3–31.

Wilson, M.D., 1992. Inherited grain-rimming clays in sandstones from eolian and shelf environments: their origin and control on reservoir properties. In: Houseknecht, D.W., Pittman, E.D., Keller, W.D.F. (Eds.), Origin, Diagenesis, and Petrophysics of Clay Minerals in Sandstones. SEPM, Special Publication, vol. 47, pp. 209–225.

Worden, R.H., Burley, S.D., 2003. Sandstone diagenesis: from sand to stone. In: Burley, S.D., Worden, R.H. (Eds.), Clastic Diagenesis: Recent and Ancient. International Association of Sedimentologists, vol. 4. Blackwells, Oxford, pp. 3–44.

Worden, R.H., Mayall, M., Evans, I.J., 2000. The effect of ductile compaction and quartz cementation on porosity and permeability in Tertiary clastics, South China Sea: prediction of reservoir quality. American Association of Petroleum Geologists Bulletin 84, 345–359.

Worden, R.H., Morad, S., 2000. Quartz cementation in oil field sandstones: a review of the key controversies. In: Worden, R.H., Morad, S. (Eds.), Quartz Cementation in Sandstones. International Association of Sedimentologists Special Publication 29. Blackwell Science, pp. 1–20.

Worden, R.H., Morad, S., 2003. Clay minerals in sandstones: controls on formation, distribution and evolution. In: Worden, R.H., Morad, S. (Eds.), Clay Mineral Cements in Sandstones. International Association of Sedimentologists Special Publication 34. Blackwell Publishing, pp. 3–41.

Worden, R.H., Oxtoby, N.H., Smalley, P.C., 1998. Can oil emplacement prevent quartz cementation in sandstones? Petroleum Geoscience 4, 129–138.

Yurkova, R.M., 1970. Comparison of post-sedimentary alterations of oil-, gas- and water-bearing rocks. Sedimentology 15, 53–68.

Zviagina, B.B., McCarty, D.K., Srodon, J., Drits, V.A., 2004. Interpretation of infrared spectra of dioctahedral smectites in the region of the OH-stretching vibrations. Clays and Clay Minerals 52, 399–410.